ADVANCES IN ELECTRONIC PACKAGING 1997

PROCEEDINGS OF THE PACIFIC RIM/ASME INTERNATIONAL INTERSOCIETY ELECTRONIC & PHOTONIC PACKAGING CONFERENCE
INTERPACK '97

Volume 2

presented at
The Pacific Rim/ASME International Intersociety Electronic
and Photonic Packaging Conference
June 15–19, 1997
Kohala Coast, Hawaii

sponsored by
The Electrical and Electronic Packaging Division, ASME

edited by
E. Suhir
Lucent Technologies

M. Shiratori
Yokohama National University

Y. C. Lee
G. Subbarayan
University of Colorado

THE AMERICAN SOCIETY OF MECHANICAL ENGINEERS
UNITED ENGINEERING CENTER • 345 EAST 47TH STREET • NEW YORK N.Y. 10017

DESIGN AND CALIBRATION OF OPTIMIZED (111) SILICON STRESS SENSING TEST CHIPS

J. C. Suhling, R. C. Jaeger, S. T. Lin, A. K. M. Mian, and R. A. Cordes
Departments of Mechanical and Electrical Engineering, and
Alabama Microelectronics Science and Technology Center
Auburn University
Auburn, AL 36849

B. M. Wilamowski
Department of Electrical Engineering
University of Wyoming
Laramie, WY 82071

ABSTRACT

The (111) surface of silicon offers unique advantages for fabrication of piezoresistive stress sensors. Resistive sensor elements fabricated on this particular surface respond to all six components comprising the state of stress. Hence, a multi-element rosette has the capability of measuring the complete stress state at a point in the material. Four of the stress component measurements are temperature compensated. This is in contrast to standard sensors fabricated on traditional (100) silicon, where only four stress components can be measured (two in a temperature compensated manner). Several generations of (111) silicon test chips have been designed, fabricated, and calibrated to demonstrate the capabilities of these advanced sensors.

INTRODUCTION

Piezoresistive stress sensors are powerful tools for experimental analysis of stress in electronic packages. As depicted in Figure 1, resistive rosette elements in IC die are characterized before and after electronic packaging, and the results are then used to extract various components of the six-component stress state on the surface of the die. Sensors on the (100) silicon surface have been used by many researchers, but these sensor elements respond only to four components of the complete stress state (Bittle, et al., 1991) (Jaeger, et al., 1994a, 1994b) (Suhling, et al., 1994a) (Cordes, et al., 1995a). In particular, the (100) devices do not respond to the out-of-plane shear stresses associated with delamination, passivation cracking, and metal shearing that can occur at the die surface with an electronic package. In addition, only two of these four stress components can be measured in a highly accurate temperature compensated manner (Jaeger et al., 1993, 1994a, 1994b) (Suhling, et al., 1994a) (Cordes, et al., 1995a).

It has been shown theoretically that piezoresistive sensor elements on the (111) surface respond to all six components of the stress state, and a six-element complete stress state sensor rosette was proposed for fabrication using (111) silicon (Bittle, et al., 1991), (Suhling, et al., 1994c). Since then we have used sophisticated symbolic computer analysis to prove that the (111) surface is in fact the best of any possible silicon orientation for sensor fabrication, as it provides temperature compensated evaluation of four of six stress-state quantities (Cordes, et al., 1995a). No other silicon surface can do as well. It is fortuitous that (111) silicon material is one of the commonly used orientations, and hence is readily available. With careful attention to temperature measurement during sensor application, (111) piezoresistive sensor test chips can be used to extract the complete state of stress at points in the surface of the die. No other type of known sensor or technique is capable of measuring the complete stress state with in an electronic package or other structure.

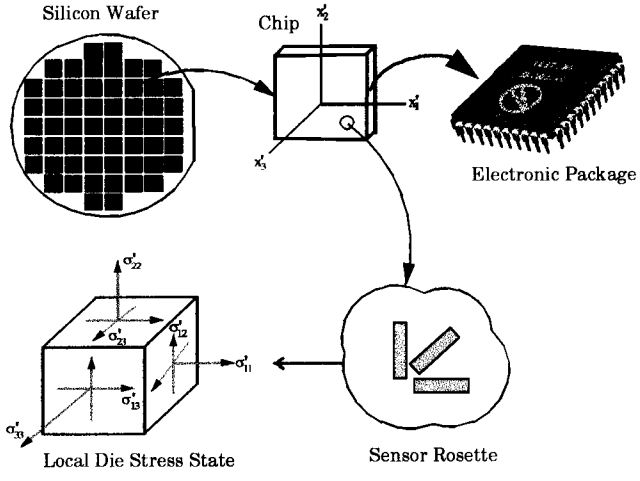

Figure 1 - Stress Sensors in Electronic Packaging

(111) SILICON PIEZORESISTIVITY THEORY

A general (111) silicon wafer is shown in Figure 2. The surface of the wafer is a (111) plane, and the [111] direction is normal to the wafer plane. The principal crystallographic axes x_1 = [100], x_2 =

[010], and x_3 = [001] do not lie in the wafer plane and have not been indicated. It is convenient to work in an off-axis primed wafer coordinate system where the axes x'_1, x'_2 are parallel and perpendicular to the primary wafer flat. Using the general theory of piezoresistivity (Bittle, et al., 1991) (Cordes, et al., 1995a), the resistance change of an arbitrarily oriented in-plane sensor can be expressed in terms of the stress components resolved in this natural wafer coordinate system:

$$\begin{aligned}\frac{\Delta R}{R} &= [B_1\sigma'_{11} + B_2\sigma'_{22} + B_3\sigma'_{33} + 2\sqrt{2}(B_2 - B_3)\sigma'_{23}]\cos^2\phi \\ &+ [B_2\sigma'_{11} + B_1\sigma'_{22} + B_3\sigma'_{33} - 2\sqrt{2}(B_2 - B_3)\sigma'_{23}]\sin^2\phi \\ &+ [2\sqrt{2}(B_2 - B_3)\sigma'_{13} + (B_1 - B_2)\sigma'_{12}]\sin 2\phi \\ &+ [\alpha_1 T + \alpha_2 T^2 + \ldots]\end{aligned} \tag{1}$$

where ϕ is again the angle between the x'_1-axis and the resistor orientation. The coefficients

$$\begin{aligned}B_1 &= \frac{\pi_{11} + \pi_{12} + \pi_{44}}{2} \\ B_2 &= \frac{\pi_{11} + 5\pi_{12} - \pi_{44}}{6} \\ B_3 &= \frac{\pi_{11} + 2\pi_{12} - \pi_{44}}{3}\end{aligned} \tag{2}$$

are a set of linearly independent temperature dependent combined piezoresistive parameters related to the three unique piezoresistive coefficients for silicon $(\pi_{11},\pi_{12},\pi_{44})$. These parameters must be calibrated before stress component values can be extracted from resistance change measurements. Equation (1) indicates that the resistance change for a resistor in the (111) plane is dependent on all six of the unique stress components. Therefore, the potential exists for developing a sensor rosette which can measure the complete three-dimensional state of stress at points on the surface of a die.

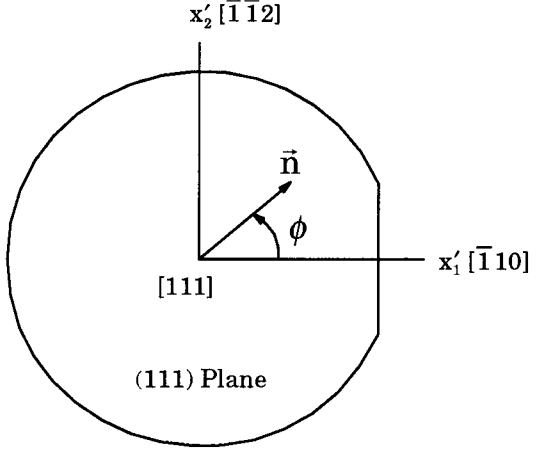

Figure 2 - (111) Silicon Wafer

Optimized sensors on (111) silicon are capable of measuring four temperature compensated combined stress components (Cordes, et al., 1995a). In this discussion, temperature compensated refers to the ability to extract the stress components directly from the resistance change measurements (without the need to know the temperature change T). This is particularly important attribute, given the large errors which can be introduced into non-temperature compensated stress sensor data when the temperature change T is not precisely known (Jaeger, et al., 1993). The four stress components which can be measured in a temperature compensated manner using (111) silicon sensors are the three shear stress components and the difference of the in-plane normal stress components.

OPTIMIZED ROSETTES

Complete stress state extraction using a (111) silicon rosette requires six independent sensor measurements. Fortunately, the three piezoresistive coefficients of silicon are different for n- and p-type material. The basic six element (111) sensor rosette initially proposed by Bittle, et al. (1991) uses three n- and three p-type resistors oriented at 0, 45° and 90° relative to the wafer flat, and can be used to extract all six stress components. However, we have discovered that the eight-element rosette in Figure 3 offers inherent advantages in stress-state extraction. This rosette contains p-type and n-type sensor sets, each with resistor elements making angles of $\phi = 0, \pm 45, 90°$ with respect to the x'_1-axis. Repeated application of eq. (1) to each of the piezoresistive sensing elements leads to the following expressions for the stress-induced resistance changes:

$$\begin{aligned}\frac{\Delta R_1}{R_1} &= B_1^n\sigma'_{11} + B_2^n\sigma'_{22} + B_3^n\sigma'_{33} + 2\sqrt{2}(B_2^n - B_3^n)\sigma'_{23} \\ &+ [\alpha_1^n T + \alpha_2^n T^2 + \ldots] \\ \frac{\Delta R_2}{R_2} &= \left(\frac{B_1^n + B_2^n}{2}\right)(\sigma'_{11} + \sigma'_{22}) + B_3^n\sigma'_{33} + 2\sqrt{2}(B_2^n - B_3^n)\sigma'_{13} \\ &+ (B_1^n - B_2^n)\sigma'_{12} + [\alpha_1^n T + \alpha_2^n T^2 + \ldots] \\ \frac{\Delta R_3}{R_3} &= B_2^n\sigma'_{11} + B_1^n\sigma'_{22} + B_3^n\sigma'_{33} - 2\sqrt{2}(B_2^n - B_3^n)\sigma'_{23} \\ &+ [\alpha_1^n T + \alpha_2^n T^2 + \ldots] \\ \frac{\Delta R_4}{R_4} &= \left(\frac{B_1^n + B_2^n}{2}\right)(\sigma'_{11} + \sigma'_{22}) + B_3^n\sigma'_{33} - 2\sqrt{2}(B_2^n - B_3^n)\sigma'_{13} \\ &- (B_1^n - B_2^n)\sigma'_{12} + [\alpha_1^n T + \alpha_2^n T^2 + \ldots] \\ \frac{\Delta R_5}{R_5} &= B_1^p\sigma_{11} + B_2^p\sigma'_{22} + B_3^p\sigma'_{33} + 2\sqrt{2}(B_2^p - B_3^p)\sigma'_{23} \\ &+ [\alpha_1^p T + \alpha_2^p T^2 + \ldots] \\ \frac{\Delta R_6}{R_6} &= \left(\frac{B_1^p + B_2^p}{2}\right)(\sigma'_{11} + \sigma'_{22}) + B_3^p\sigma'_{33} + 2\sqrt{2}(B_2^p - B_3^p)\sigma'_{13} \\ &+ (B_1^p - B_2^p)\sigma'_{12} + [\alpha_1^p T + \alpha_2^p T^2 + \ldots] \\ \frac{\Delta R_7}{R_7} &= B_2^p\sigma'_{11} + B_1^p\sigma'_{22} + B_3^p\sigma'_{33} - 2\sqrt{2}(B_2^p - B_3^p)\sigma'_{23} \\ &+ [\alpha_1^p T + \alpha_2^p T^2 + \ldots] \\ \frac{\Delta R_8}{R_8} &= \left(\frac{B_1^p + B_2^p}{2}\right)(\sigma'_{11} + \sigma'_{22}) + B_3^p\sigma'_{33} - 2\sqrt{2}(B_2^p - B_3^p)\sigma'_{13} \\ &- (B_1^p - B_2^p)\sigma'_{12} + [\alpha_1^p T + \alpha_2^p T^2 + \ldots]\end{aligned} \tag{3}$$

Superscripts n and p are used on the combined piezoresistive coefficients to denote n-type and p-type resistors, respectively.

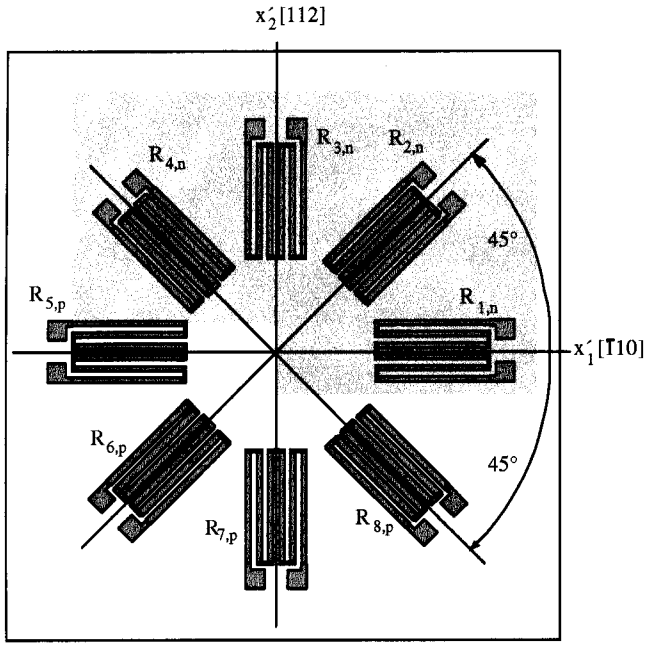

Figure 3 - Optimized Eight Element Rosette on (111) Silicon

For an arbitrary state of stress, these expressions can be inverted to solve for the six stress components in terms of the measured resistance changes:

$$\sigma'_{11} = \frac{(B_3^p - B_2^p)\left[\frac{\Delta R_1}{R_1} - \frac{\Delta R_3}{R_3}\right] - (B_3^n - B_2^n)\left[\frac{\Delta R_5}{R_5} - \frac{\Delta R_7}{R_7}\right]}{2[(B_2^p - B_1^p)B_3^n + (B_1^p - B_3^p)B_2^n + (B_3^p - B_2^p)B_1^n]} + \frac{B_3^p\left[\frac{\Delta R_1}{R_1} + \frac{\Delta R_3}{R_3} - 2\alpha_1^n T\right] - B_3^n\left[\frac{\Delta R_5}{R_5} + \frac{\Delta R_7}{R_7} - 2\alpha_1^p T\right]}{2[(B_1^n + B_2^n)B_3^p - (B_1^p + B_2^p)B_3^n]}$$

$$\sigma'_{22} = -\frac{(B_3^p - B_2^p)\left[\frac{\Delta R_1}{R_1} - \frac{\Delta R_3}{R_3}\right] - (B_3^n - B_2^n)\left[\frac{\Delta R_5}{R_5} - \frac{\Delta R_7}{R_7}\right]}{2[(B_2^p - B_1^p)B_3^n + (B_1^p - B_3^p)B_2^n + (B_3^p - B_2^p)B_1^n]} + \frac{B_3^p\left[\frac{\Delta R_1}{R_1} + \frac{\Delta R_3}{R_3} - 2\alpha_1^n T\right] - B_3^n\left[\frac{\Delta R_5}{R_5} + \frac{\Delta R_7}{R_7} - 2\alpha_1^p T\right]}{2[(B_1^n + B_2^n)B_3^p - (B_1^p + B_2^p)B_3^n]} \quad (4)$$

$$\sigma'_{33} = \frac{-(B_1^p + B_2^p)\left[\frac{\Delta R_1}{R_1} + \frac{\Delta R_3}{R_3} - 2\alpha_1^n T\right] + (B_1^n + B_2^n)\left[\frac{\Delta R_5}{R_5} + \frac{\Delta R_7}{R_7} - 2\alpha_1^p T\right]}{2[(B_1^n + B_2^n)B_3^p - (B_1^p + B_2^p)B_3^n]}$$

$$\sigma'_{13} = \frac{\sqrt{2}}{8}\left[\frac{(B_2^p - B_1^p)\left[\frac{\Delta R_4}{R_4} - \frac{\Delta R_2}{R_2}\right] - (B_2^n - B_1^n)\left[\frac{\Delta R_8}{R_8} - \frac{\Delta R_6}{R_6}\right]}{(B_2^p - B_1^p)B_3^n + (B_1^p - B_3^p)B_2^n + (B_3^p - B_2^p)B_1^n}\right]$$

$$\sigma'_{23} = \frac{\sqrt{2}}{8}\left[\frac{-(B_2^p - B_1^p)\left[\frac{\Delta R_1}{R_1} - \frac{\Delta R_3}{R_3}\right] + (B_2^n - B_1^n)\left[\frac{\Delta R_5}{R_5} - \frac{\Delta R_7}{R_7}\right]}{(B_2^p - B_1^p)B_3^n + (B_1^p - B_3^p)B_2^n + (B_3^p - B_2^p)B_1^n}\right]$$

$$\sigma'_{12} = \frac{-(B_3^p - B_2^p)\left[\frac{\Delta R_4}{R_4} - \frac{\Delta R_2}{R_2}\right] + (B_3^n - B_2^n)\left[\frac{\Delta R_8}{R_8} - \frac{\Delta R_6}{R_6}\right]}{2[(B_2^p - B_1^p)B_3^n + (B_1^p - B_3^p)B_2^n + (B_3^p - B_2^p)B_1^n]}$$

It can be seen that the three shear stresses are temperature compensated (they can be calculated directly from the resistance changes without knowing T). A fourth temperature compensated quantity can be obtained by subtracting the expressions for the in-plane normal stresses σ'_{11} and σ'_{22} in eq. (4):

$$\sigma'_{11} - \sigma'_{22} = \frac{(B_3^p - B_2^p)\left[\frac{\Delta R_1}{R_1} - \frac{\Delta R_3}{R_3}\right] - (B_3^n - B_2^n)\left[\frac{\Delta R_5}{R_5} - \frac{\Delta R_7}{R_7}\right]}{[(B_2^p - B_1^p)B_3^n + (B_1^p - B_3^p)B_2^n + (B_3^p - B_2^p)B_1^n]} \quad (5)$$

From the resistor change equations in eq. (3) and the resulting the stress-component equations in eqs. (4,5), it can be seen that the 0-90° and ±45° resistor changes appear grouped in pairs and quads. Thus, the eight-element rosette facilitates bridge-type measurements for the temperature compensated terms.

TEST CHIP DESIGNS

Several generations of (111) stress sensor chips have been designed, fabricated and characterized for use in packaging studies. These test die contain an array of the optimized eight element dual polarity measurement rosettes shown in Figure 3, and either perimeter pads suitable for wire bonding or area array pads for flip chip applications. The fabrication processes used only ion-implantation to achieve the best possible resistor matching and uniformity. Careful layout techniques were used to maximize matching and to minimize sensitivity to mask misalignment during fabrication.

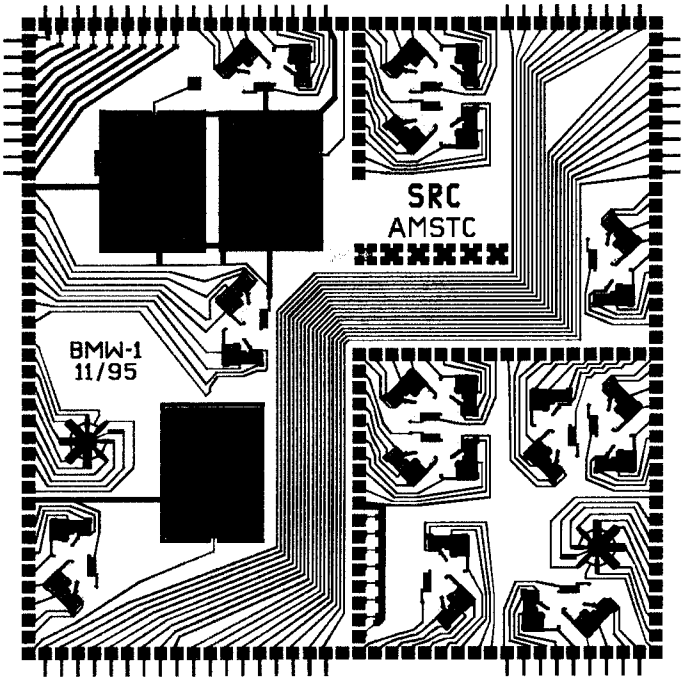

Figure 4 - BMW1 Test Chip.

The basic die image of the first generation BMW1 test chip is shown in Figure 4. This 200 x 200 mil die contains 12 of the eight-element rosettes discussed above. A typical rosette layout and its connection to the perimeter bond pads is shown in Figure 5. The wafer can be cut into larger chips on any 200 mil increment in either direction. The repeated basic die images are interconnected through the scribe areas on the wafer using the shorting bars extending from the pads (see Figure 4). These inter-chip connections provide access to interior sensors (from the outer perimeter pads) on larger composite die up to 1200 x 1200 mils in size. For example, Figure 6 shows the rosette locations (shaded) which are accessible from the perimeter pads of a 6 x 6 array of the basic die image (1200 mil x 1200 mil die).

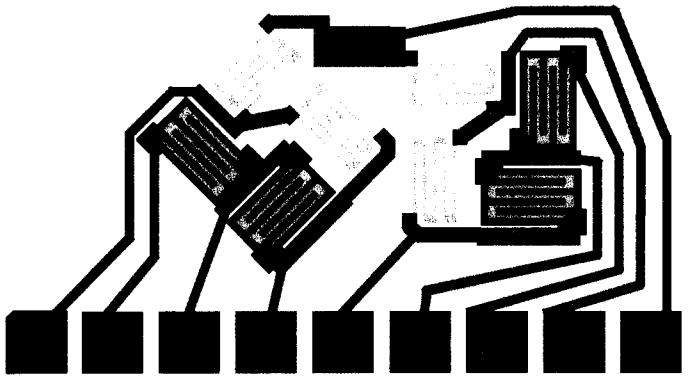

Figure 5 - BMW1 Rosette Schematic

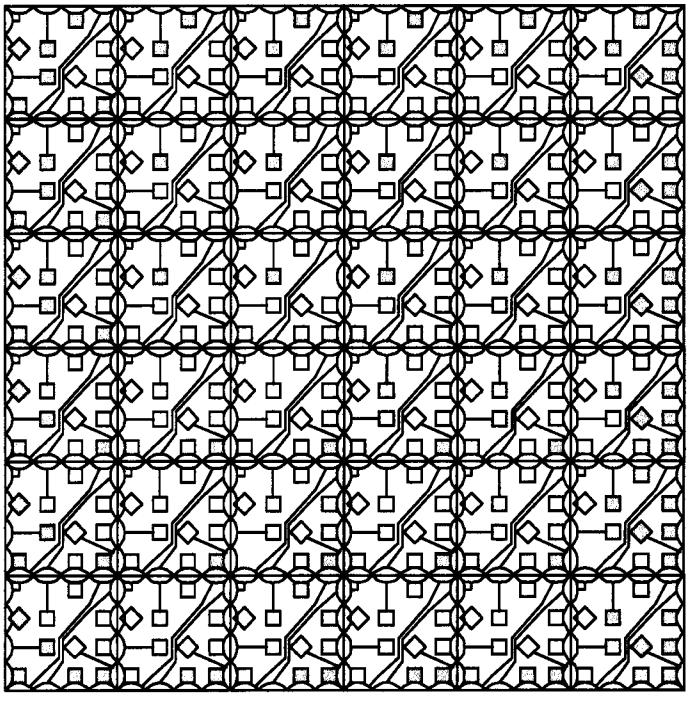

Figure 6 - Sensor Access in a Large 6 x 6 Chip Array
(1200 mil x 1200 mil Die)

The rosette locations of the BMW1 chip were carefully chosen to map the surface stress using symmetry (when it exists). Figure 7 presents an example of using this symmetry to map the surface of a 2 x 2 array of the BMW1 die.

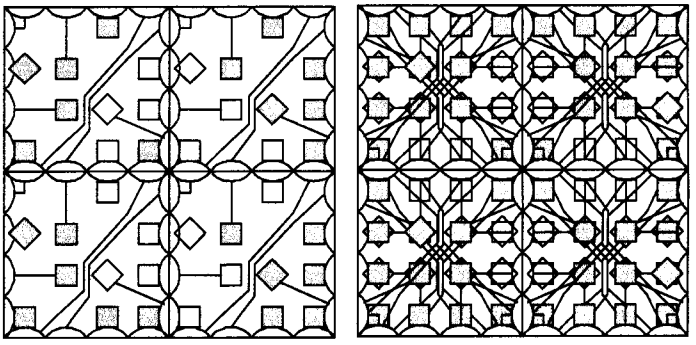

No Symmetry Symmetry Assumed

Figure 7 - Surface Mapping in a 2 x 2 Chip Array
(400 mil x 400 mil Die)

Our second generation design, the BMW2 die, is shown in Figure 8. It incorporates 12 eight-element rosettes, diodes at each rosette site for temperature measurement, and additional calibration sites and process test structures. The eight-element rosettes are interconnected as half-bridge circuits (see Figure 9), which optimizes the number of pads needed to completely access all sensors in a given rosette. The implantation profiles were chosen based upon the results of a parametric process study that was done as part of the fabrication of the BMW1 wafers. Doping levels for both resistor types were in the low 10^{18} $1/cm^3$ range, and the nominal resistor values were designed to be approximately 12-15 kΩ.

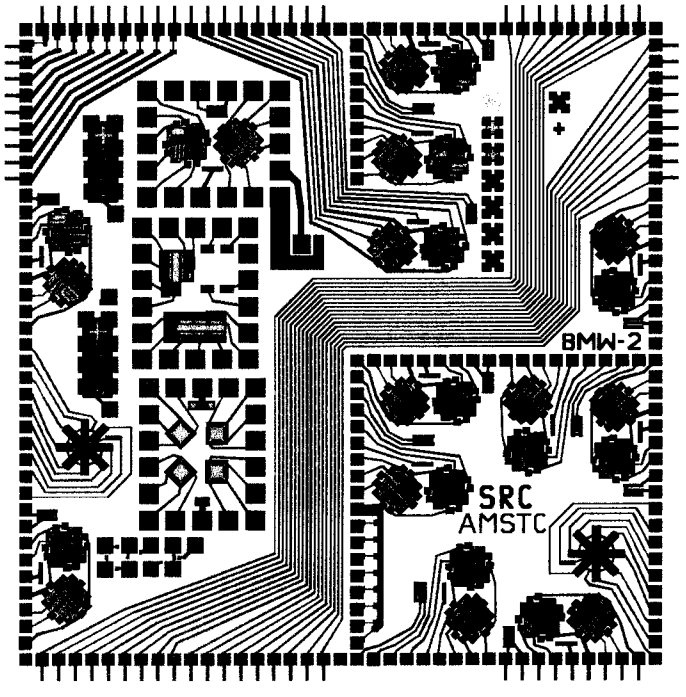

Figure 8 - BMW2 Test Chip.

Two additional (111) silicon test chip designs have been developed for direct chip attach (flip-chip) applications (BMW3 and BMW4 test

chips). Each has an area array of 4 x 4 mil pads; one on 20 mil centers, the other on 9 mil centers. In the flip-chip designs, the optimized eight element rosettes are placed between the pads as well as directly under pads. This facilitates studies of the out-of-plane shear stresses transmitted to the die by the solder bumps or the underfill encapsulant. The basic repeated image on the wafer are small sensing cells, which allows flip-chip test die of almost any preferred size to be cut from the wafers. A schematic of the BMW3 sensing cell is shown in Figure 10.

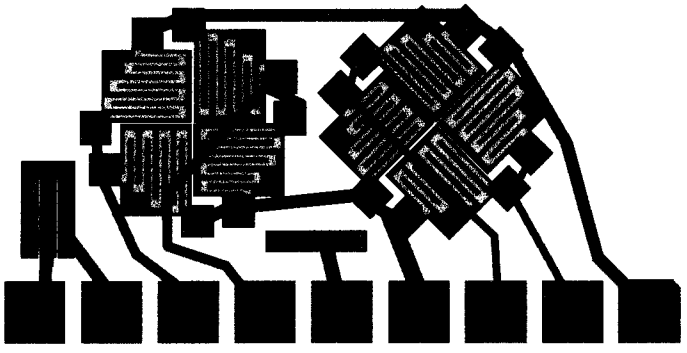

Figure 9 - BMW2 Rosette Schematic Using Half Bridges

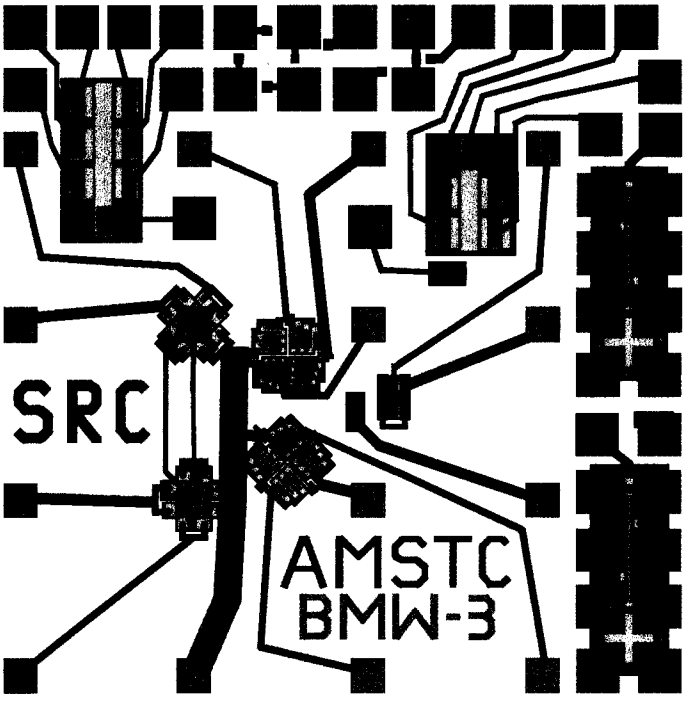

Figure 10 - BMW3 Flip Chip Sensing Cell

CALIBRATION

The expressions in eq. (3) indicate that a calibration procedure must be performed to determine all six of the combined piezoresistive parameters B_1^n, B_2^n, B_3^n, B_1^p, B_2^p, B_3^p prior to using the eight element rosettes on any of the test chips for stress measurement. A combination of uniaxial and hydrostatic pressure testing can be utilized to complete this task. For example, if a known uniaxial stress $\sigma'_{11} = \sigma$ is applied in the x_1'-direction, the expressions in eq. (3) for the 0-90° oriented sensors yield the following resistance changes:

$$\frac{\Delta R_1}{R_1} = B_1^n\sigma + \alpha_1^n T \qquad \frac{\Delta R_3}{R_3} = B_2^n\sigma + \alpha_1^n T$$
$$\frac{\Delta R_5}{R_5} = B_1^p\sigma + \alpha_1^p T \qquad \frac{\Delta R_7}{R_7} = B_2^p\sigma + \alpha_1^p T \tag{6}$$

From these expressions, it is clear that the constants B_1^n, B_2^n, B_1^p, B_2^p can be easily determined through a controlled isothermal application of uniaxial stress to a sensor rosette while monitoring the resulting resistance changes. If a sensor rosette are subjected to hydrostatic pressure $(\sigma'_{11} = \sigma'_{22} = \sigma'_{33} = -p)$, the relations in eq. (3) give:

$$\frac{\Delta R_1}{R_1} = \frac{\Delta R_2}{R_2} = \frac{\Delta R_3}{R_3} = \frac{\Delta R_4}{R_4} = -[B_1^n + B_2^n + B_3^n]p + \alpha_1^n T$$
$$\frac{\Delta R_5}{R_5} = \frac{\Delta R_6}{R_6} = \frac{\Delta R_7}{R_7} = \frac{\Delta R_8}{R_8} = -[B_1^p + B_2^p + B_3^p]p + \alpha_1^p T \tag{7}$$

Therefore, the combinations $(B_1^n + B_2^n + B_3^n)$ and $(B_1^p + B_2^p + B_3^p)$ can be evaluated through a controlled isothermal application of a hydrostatic pressure to a sensor rosette while monitoring the resulting resistance changes. The individual values of B_3^n and B_3^p can then be obtained by combining the hydrostatic pressure calibration results with the uniaxial stress calibration results.

Four-point bending (Jaeger, et al., 1992), wafer-level (Suhling, et al., 1994b) (Cordes, et al., 1995b), and hydrostatic calibration (Kang, 1997) techniques were used to determine the six piezoresistive coefficients needed to calculate stress states from the normalized resistor changes of the eight rosette elements. The four point bending and wafer-level techniques subject the die to in-plane stress states, so that only constants B_1 and B_2 can be evaluated. In the four point bending method, a rectangular strip containing a row of chips is cut from a wafer and is loaded in a four point bending beam fixture to generate uniaxial stress states (see Figure 11). As observed above in eq. (6), this technique allowed coefficients B_1 and B_2 to be measured. In the wafer-level calibration method, the wafer itself was supported on a vacuum chuck, and air inside the chamber was removed causing a uniformly distributed load to be applied to the wafer (see Figure 12). This technique also allowed coefficients B_1 and B_2 to be measured, providing a check on the four point bending data. Sample calibration measurements for the BMW1 test chip appear in Figures 13-14 for the four point bending method, and in Figure 15 for the wafer-level technique.

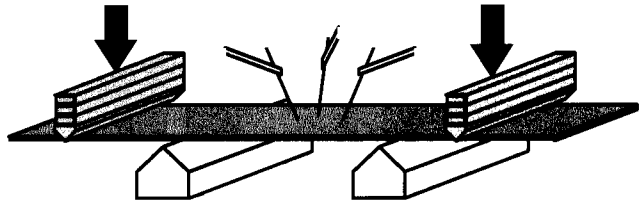

Figure 11 - Four Point Bending Calibration

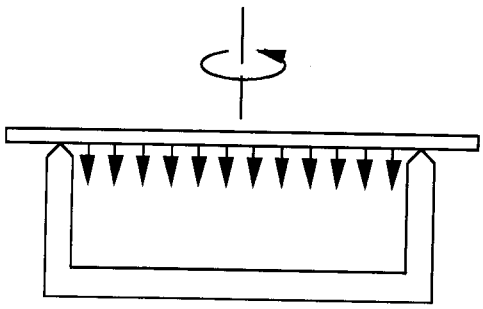

Figure 12 - Wafer-Level Calibration Schematic

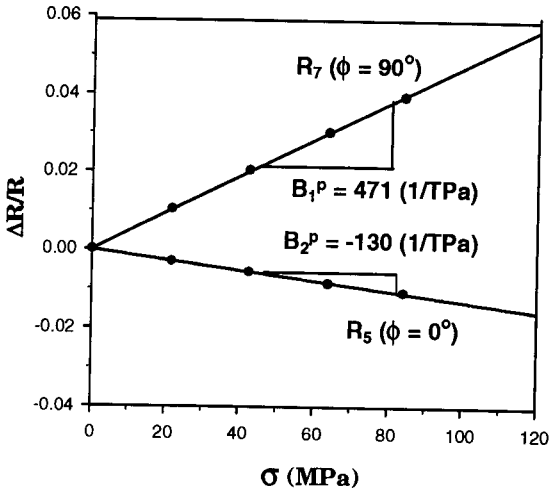

Figure 13 - Typical Four Point Bending Results
(P-Type Resistors, 8 Element Rosette)

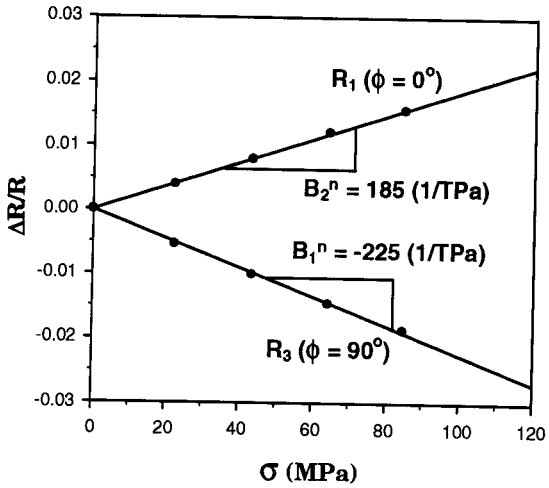

Figure 14 - Typical Four Point Bending Results
(N-Type Resistors, 8 Element Rosette)

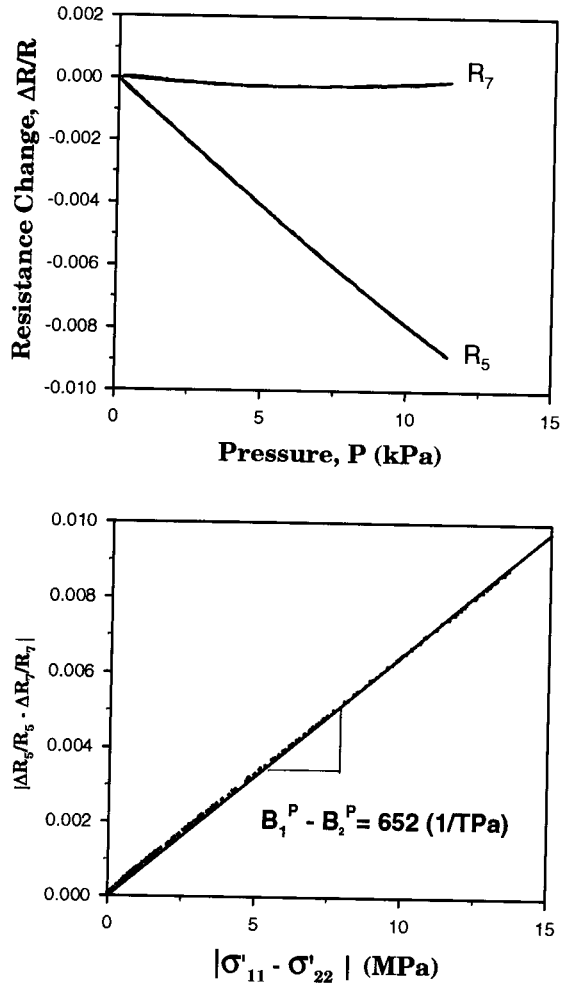

Figure 15 - Typical Wafer-Level Calibration Data
(P-Type Resistors, 8 Element Rosette)

It can be easily seen using eq. (3) that characterization of material constant B_3 requires the die to be subjected to a controlled stress state which has non-zero out-of-plane normal or shear stresses. Hydrostatic calibration has proven to be the most expedient method to satisfy this condition. In the case of hydrostatic calibration, a high capacity pressure vessel was used to subject a single die to triaxial compression. The theoretical considerations presented in eq. (7) has demonstrated that the slope of the resistance change versus pressure response is $(B_1 + B_2 + B_3)$ for a sensor at any orientation. Figure 16 shows typical hydrostatic calibration data obtained using the BMW1 test chip.

A summary of the calibration results for the BMW1 die are given in Figure 17. The first row gives the values of the piezoresistive coefficients obtained from an average of at least 10 rosette sites. These values are approximately 2/3 of those for lightly doped material that are given in the last row of the table. The lightly doped values place an upper bound on the magnitudes of the piezoresistive coefficients. Relatively high sensitivity has been obtained by carefully tailoring the impurity doses used in the ion-implanted resistors. Note also that the pressure coefficients are quite low as expected.

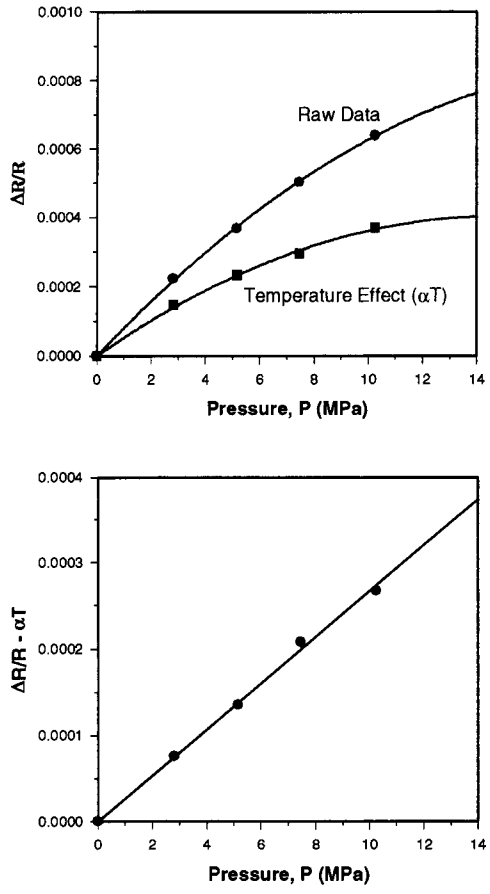

Figure 16 - Typical Hydrostatic Calibration Data (P-Type Resistor

Measured Piezoresistive Coefficients for the BMW1 ($\times 10^{-12}$ Pa^{-1}) (Average Values Considering 10 Rosette Sites)					
B_1^p	B_2^p	$B_1^p + B_2^p + B_3^p$	B_1^n	B_2^n	$B_1^n + B_2^n + B_3^n$
464	-130	27	-220	193	36
Values for Lightly Doped Silicon					
718	-228	44	-311	298	48

Figure 17 - Tabulation of Calibration Data

CONCLUSIONS

New optimized complete stress state test chips have been fabricated using (111) silicon. Eight-element rosettes are used in half-bridge configurations to simplify stress measurements. The process design and layout have been optimized to provide high sensitivity to stress and to improve resistor matching. Calibration results have shown that high sensitivity and good matching are both achieved. These die have been successfully used for packaging stress measurements, and have produced the first measurement of the complete stress state in any material (see Suhling, et al., 1997).

Information concerning the availability of these stress test chips can be obtained from the Test Chip Division of the Alabama Microelectronics Science and Technology Center (+1-334-844-1871).

ACKNOWLEDGMENTS

This work has been supported by the Semiconductor Research Corporation.

REFERENCES

Bittle, D. A., Suhling, J. C., Beaty, R. E., Jaeger, R. C. and Johnson, R. W., 1991, "Piezoresistive Stress Sensors for Structural Analysis of Electronic Packages," *Journal of Electronic Packaging*, Vol. 113(3), pp. 203-215.

Cordes, R. A., Suhling, J. C., Kang, Y. and Jaeger, R. C., 1995a, "Optimal Temperature Compensated Piezoresistive Stress Sensor Rosettes," in the *Proceedings of the Symposium on Applications of Experimental Mechanics to Electronic Packaging*, American Society of Mechanical Engineers, EEP-Vol. 13, pp. 109-116.

Cordes, R. A., Suhling, J. C., Kang, Y. and Jaeger, R. C., 1995b, "Application of a Wafer-Level Calibration Technique for Stress Sensing Test Chips," in the *Proceedings of the Symposium on Applications of Experimental Mechanics to Electronic Packaging*, American Society of Mechanical Engineers, EEP-Vol. 13, pp. 79-94.

Jaeger, R. C., Beaty, R. E., Suhling, J. C., Johnson, R. W. and Butler, R. D., 1992, "Evaluation of Piezoresistive Coefficient Variation in Silicon Stress sensors Using a Four-Point Bending Test Fixture," *IEEE Transactions on Components, Hybrids, and Manufacturing Technology (CHMT)*, Vol. 15(5), pp. 904-914.

Jaeger, R. C., Suhling, J. C. and Ramani, R., 1993, "Thermally Induced Errors in the Application of Silicon Piezoresistive Stress Sensors," in the *Advances in Electronic Packaging 1993 - Proceedings of the 1993 ASME International Electronic Packaging Conference*, Binghamton, NY, September 29-October 2, 1993, pp. 457-470.

Jaeger, R. C., Suhling, J. C. and Ramani, R., 1994a, "Errors Associated with the Design, Calibration of Piezoresistive Stress Sensors in (100) Silicon," *IEEE Transactions on Components, Packaging, and Manufacturing Technology - Part B: Advanced Packaging*, Vol. 17(1), pp. 97-107.

Jaeger, R. C., Suhling, J. C., Ramani, R. and Anderson, A. A., 1994b, "A (100) Silicon Stress Test Chip with Optimized Piezoresistive Sensor Rosettes," *Proceedings of the 1994 Electronic Components and Technology Conference (ECTC)*, Washington, DC, May 1-4, 1994, pp. 741-749.

Kang, Y., 1997, *Piezoresistive Stress Sensors for Advanced Semiconductor Materials*, Ph.D. Dissertation, Auburn University

Suhling, J. C., Jaeger, R. C. and Anderson, A. A., 1994a, "Optimized Stress Sensors for Application to Electronic Packaging," *Proceedings of the International Conference on Advances in Engineering Measurements*, University of Edinburgh, Scotland, pp. 9-15.

Suhling, J. C., Cordes, R. A., Kang, Y. L., and Jaeger, R. C., 1994b, "Wafer-Level Calibration of Stress Sensing Test Chips," in the *Proceedings of the 44th Electronic Components and Technology Conference (ECTC)*, pp. 1058-1070.

Suhling, J. C., Jaeger, R. C. and Ramani, R., 1994c, "Stress Measurement Using 0-90 Piezoresistive Rosettes on (111) Silicon," in *Mechanics and Materials for Electronic Packaging: Volume 1 - Design and Process Issues in Electronic Packaging*, American Society of Mechanical Engineers, AMD-Vol. 195, pp. 65-73.

Suhling, J. C., Jaeger, R. C., Lin, S. T., Moral, R. J. and Zou, Y., 1997, "Measurement of the Complete Stress State in Plastic Encapsulated Packages," to Appear in the *Proceedings of INTERpack '97*, Hawaii, HI, June 15-19, 1997.